

PROPERTIES OF THE NILI FOSSAE OLIVINE-CLAY-CARBONATE LITHOLOGY. A.J. Brown¹, R.C. Wiens², P. Pinet³, Y. Liu⁴, E. Cloutis⁵, J.M. Madariaga⁶, J.M. Comellas⁷, M. Schmidt⁸, J.I. Simon⁹, G. Poggiali¹⁰, J.D. Hernandez-Montenegro⁴, Plancius Research, MD (adrian.j.brown@nasa.gov) ²EAPS, Purdue Univ, West Lafayette, IN ³IRAP, Toulouse, France ⁴JPL, CalTech ⁵Univ Winnipeg, ⁶Univ of Basque Country, Leioa, Spain, ⁷Univ of Hawai'i, ⁸Brock Univ, Ontario, ⁹NASA JSC, Houston, TX, ¹⁰INAF, Italy.

Introduction: The *Perseverance* rover landed at Jezero crater on 18 February 2021. After landing, the rover has traveled to the “Séítah” region [1,2] and has brought us insights into the formation of the olivine-clay-carbonate bearing rocks that were previously identified from orbit [3,4]. Here we use the SuperCam VISIR and LIBS to investigate the properties of the lithology in situ and determine two things: 1) the olivine-clay-carbonate regional lithology is low in Al³⁺, which allows us to eliminate the possibility of clays which are high in Al³⁺, 2) the viscosity of the Séítah formation is as low as terrestrial dunite, which is a reasonable explanation of the cumulate and thin-layered units the rover has observed.

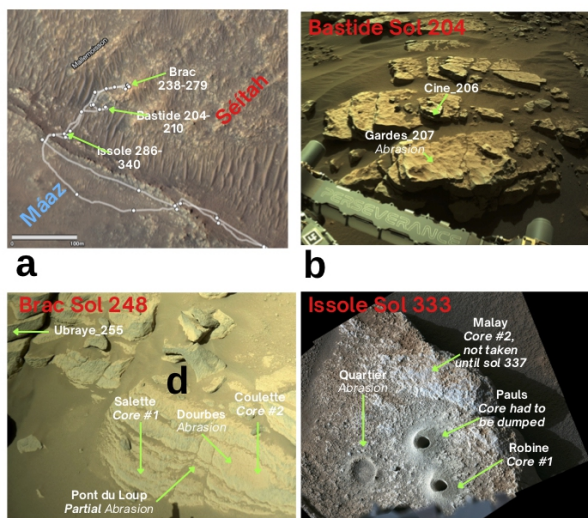


Fig. 1 Visual summary of the traverse through the Séítah formation and the three key workspaces Bastide, Brac and Issole.

SuperCam: SuperCam has been used to identify cumulate olivine and characterize its Fo# using Raman and LIBS measurements [6]. The SuperCam VISIR data set is being compared to spectral features seen from orbit by CRISM [7]. Figs 1-3 show an olivine-rich rock with a cumulate texture imaged by the SuperCam RMI and VISIR at Cine in Séítah.

CRISM: We have utilized orbital (CRISM) data with a Venn-diagrammatic approach (Figs 5-6) to determine the relationships between the olivine-clay-carbonate in the CRISM HRL40FF image.

Clay: We were able to show that clay is also present in the olivine-carbonate lithology. We have now used in situ observations to help identify the clay.

We have used the SuperCam VISIR instrument onboard the rover to observe the 2-2.5 μm region of the spectrum to look for bands indicative of clays in the olivine cumulate rocks of Séítah. Using the appearance of the 2.38 and 2.46 μm bands we have been able to narrow the search to clays with metal-OH features. Finally, we have used the SuperCam LIBS instrument to determine the low (<4 wt %) Al₂O₃ thereby allowing us to eliminate clays with aluminum in their structure. The only remaining candidates are talc and serpentine.

Viscosity: Using elemental abundances derived by the LIBS instrument on SuperCam, we have used the heuristic Bottinga-Weill approach [5] to derive the viscosity of the lava flow that emplaced the Séítah cumulate [6], and find it to be exceedingly low (Fig 4). Based on this observation, we hypothesize that the Séítah unit was formed by a flood lava similar to the Columbia Ridge basalt [7]. We hypothesize that the olivine cumulate was formed at the base of a lava lake within Jezero crater that was part of a Nili Fossae region-wide unit.

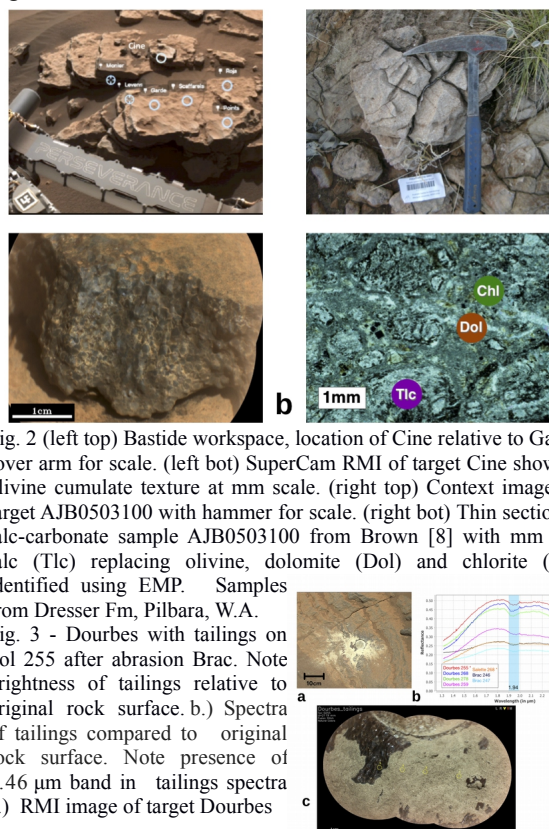


Fig. 2 (left top) Bastide workspace, location of Cine relative to Garde, rover arm for scale. (left bot) SuperCam RMI of target Cine showing olivine cumulate texture at mm scale. (right top) Context image for target AJB0503100 with hammer for scale. (right bot) Thin section of talc-carbonate sample AJB0503100 from Brown [8] with mm size talc (Tlc) replacing olivine, dolomite (Dol) and chlorite (Chl) identified using EMP. Samples from Dresser Fm, Pilbara, W.A.

Fig. 3 - Dourbes with tailings on Sol 255 after abrasion Brac. Note brightness of tailings relative to original rock surface. b.) Spectra of tailings compared to original rock surface. Note presence of 2.46 μm band in tailings spectra c.) RMI image of target Dourbes

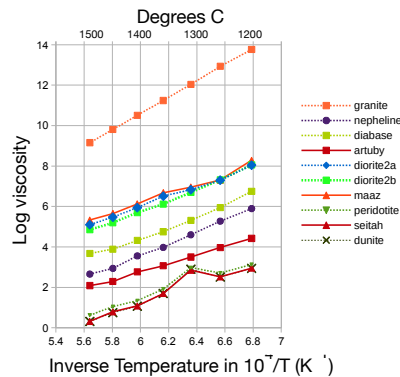


Fig 4. Arrhenius plot of Bottinga-Weill viscosity vs inverse temp. for Maaz (orange), Séítah (red) and Artuby (marone) compared to standards (dots). Note that the dunite and Séítah lines almost overlap in this plot.

What have we learned about the Olivine-clay-carbonate lithology? The olivine-clay-carbonate lithology is among the best-documented rock types in Jezero crater and the surrounding watershed [3] and is potentially among the most astrobiologically compelling units in the region [10]. From orbital VNIR reflectance spectra, the unit contains abundant olivine (Fo#45-66) in large grains (>500 μm , based on band saturation) accompanied by clay and carbonate minerals [4], and its crater retention age is ~ 3.82 Ga [11]. Several potential origins of the olivine-rich unit are possible: 1) a density segregated melt associated with a lava flow or lake; 2) a pyroclastic density current (PDC) at low temperature [11]; 3) tephra fall [12]; or 4) some combination of all of the above, see also [13]. The transition from primary volcanic deposit to the olivine-clay-carbonate could have been caused by deuteric serpentinization and talc-carbonation [8] perhaps caused by late Noachian CO_2 outgassing [14]. It is also possible that the olivine was altered to carbonate when it was exposed to a thick CO_2 -rich Noachian atmosphere [15]. Discrimination between these formation and alteration histories is critical to advancing our understanding of Noachian mantle circulation [16].

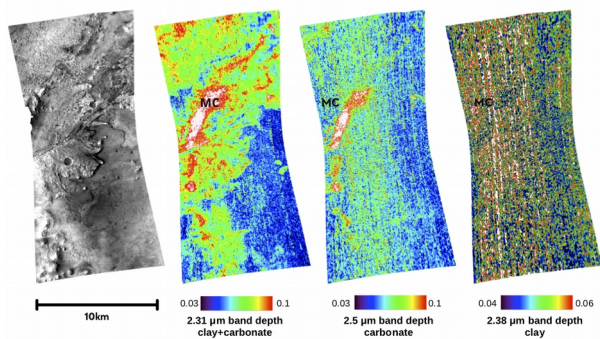
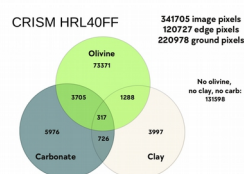


Fig 5 - HRL40FF 0.905 μm , 2.31 μm , 2.5 μm , 2.38 μm band maps. "MC" is location of marginal carbonates.

Fig 6. Venn diagram of olivine-clay-carbonate detections for HRL40FF showing pixels with olivine, clay and carbonate.



Why such thin layering and polyhedral jointing? Terrestrial komatiite sequence (usually dunite) lavas have extremely low viscosity, and provide a starting indication for what the lava emplacement mechanism must have been for the olivine-clay-carbonate layers at Séítah and beyond in Nili Fossae. The thin layering (Fig 1) probably also contributes to the draping appearance of the unit reported in [12]. In addition, polyhedral jointing is present at the top of many komatiite successions, (e.g. Dundonald Sill, Ontario) and is regarded as strong evidence of an extrusive origin [17].

Take away messages: We used CRISM and in situ data from the Mars2020 rover to examine the properties and emplacement of the olivine-clay-carbonate lithology. We have found the following:

We have calculated the viscosity of the unit based on geochemical elemental abundances of the Séítah olivine cumulate rock.

We show that clay is also present in the olivine-carbonate lithology. We used VISIR instrument to observe the 2-2.5 μm region of the spectrum to look for bands indicative of clays in the olivine cumulate rocks of Séítah.

We have used the SuperCam LIBS instrument to determine Séítah's low (<4wt %) Al_2O_3 - allowing us to eliminate clays with aluminum in their structure.

Using elemental abundances from the SuperCam LIBS, we derive the viscosity of the lava flow that emplaced the Séítah cumulate, and find it to be exceedingly low. Based on this observation, we hypothesize that the Séítah unit was formed by a flood lava similar to the Columbia Ridge basalt. We hypothesize that the olivine cumulate was formed at the base of a lava lake within Jezero crater that was part of the region-wide unit.

References: [1] Farley, K.A.+ (2020) SSR 216 [142](#) [2] Stack, K.M.+ (2020) SSR 216 [127](#) Sun, V. and Stack, K.M. USGS SIMap [#3464](#) [3] Ehlmann B.+ (2008) *Science* **322** [1828](#) Goudge, T.+(2015) *JGR* **120** [775-808](#) [4] Brown, A.J.+ (2020) *JGR* **125** [2019JE006011](#); Brown, A.J.+ (2010) *EPSL* **297** [174-182](#) [5] Bottinga and Weill, 1972 *American J. of Science* **272** [438-475](#); McGetchin and Smythe J.R. (1978) *Icarus* **34** [512-536](#) [6] Wiens, R.+ (2022) *Science Advances*, **3399**; Udry, A.+ (2022) *JGR* special section; Mandon, L.+ (2022) *JGR* special section; [7] Plescia, J. (1990) *Icarus* **88** [465-490](#) [8] Brown, A.J. (2006) [PhD thesis](#), Macquarie Univ. [9] Worster+ (1993) *JGR* **98**. [10] Horgan, B.+ (2020) *Icarus* **339** [113526](#) [11] Mandon+ (2020) *Icarus* **336** [113436](#) [12] Kremer, C.+ (2019) *Geology* **111** [E02S10](#) [13] Ravanis, E.+ (2023) this meeting [14] Grott, M.+ *EPSL* **308** [391-400](#) [15] Pollack, J.B.+ (1987) *Icarus* **71** [203-224](#) [16] Hirschmann, M.M.+Withers, A.C. *EPSL* **270** [147-155](#) Kiefer, W.S. (2003) *MAPS* **38** [1815-1832](#) [17] Arndt, N. + (2004) *Journal of Petrology* **45** [2555](#)